International Journal of Innovative Technology and Exploring Engineering (IJITEE)
ISSN: 2278-3075 (Online), Volume-9 Issue-4, February 2020

Compact Schemes for the Spatial Discretization of Linear Elliptic Partial Differential Equations

E. Dhananjaya, R. Bhuvana Vijaya

Abstract*: *A system of compact schemes used, to approximate the partial derivative $\frac{\partial^2 f}{\partial x_1^2}$ and $\frac{\partial^2 f}{\partial x_2^2}$ of Linear Elliptic Partial Differential Equations (LEPDE) ,on the non-boundary nodes, located along a particular horizontal grid line for $\frac{\partial^2 f}{\partial x_1^2}$ and along a particular vertical grid line for $\frac{\partial^2 f}{\partial x_2^2}$ of a two-dimensional structured Cartesian uniform gr.d. The aim of the numerical experiment is to demonstrate the higher order spatial accuracy and better rate of convergence of the solution, produced using the developed compact scheme. Further, these solutions are compared with the same, produced using the conventional 2^{nd} order scheme. The comparison is made, in terms of the discrete l_2 & l_∞ norms, of the true error. The true error is defined as, the difference between the computed numerical and the available exact solution, of the chosen test problems. It is computed on every non-boundary node bounded in the computational domain.

Keywords* : *Fourth order central difference based compact schemes, spatial discretization, Linear Elliptic Partial Differential Equations, Incompressible fluid flow, Explicit Scheme.

I. INTRODUCTION

Two of the most common model equations, belonging to the class of Linear Elliptic Partial Differential Equations (LEPDE) [1-3], are the Poisson and Laplace equations. The mathematical forms of these two equations, in two dimensions are given by,

$$\frac{\partial^2 f}{\partial x_1^2}+\frac{\partial^2 f}{\partial x_2^2}=g\left(x_1,x_2\right) \qquad (1.1)$$

And

$$\frac{\partial^2 f}{\partial x_1^2}+\frac{\partial^2 f}{\partial x_2^2}=0 \qquad (1.2)$$

Where $g\left(x_1,x_2\right)$ s the source term of the Poisson equation.

Equations (1.1) and (1.2) must be satisfied for all $\left(x_1,x_2\right)$ in some open domain of the plane Ω_d . The boundary conditions are defined, in terms of the function and/or its derivatives, on $\partial\Omega_d$ which represents the boundary of the domain. A few examples of the physical phenomena governed by these equations are the steady state heat conduction, potential flows and pressure Poisson equation related to incompressible flows etc.

Generally, the equations of elliptic nature represent the steady state behavior of a function, in some region of space, of the time dependent physical problems. Suppose, the source term and the boundary conditions of the elliptic equations are independent of time, then, there is a possibility of steady state solution to exist. In the following subsection, the derivation of the compact scheme for Poisson and Laplace equations and the corresponding numerical algorithm developed to solve them are explained.

Explained details about a typical two-dimensional structured Cartesian uniform grid for spatial descretization [4-7].

Developed the higher order compact schemes (HOCS) suitable to the discretization of Poisson and Laplace equations from the central difference-based compact schemes (CDCS) [8-11] and upwind difference-based compact schemes (UDCS) [12-16] Finally in the last part of this section, the developed compact 4^{th} order schemes are tested using two test problems subjected to the Dirichlet boundary conditions (one each for Laplace and Poisson equations).

II. DETAILS OF THE GRID USED FOR SPATIAL DISCRETIZATION

The schematic of the grid used, to map a rectangular computational domain is shown, in the Figure 1.1. This particular mesh is conceived to be a network, obtained by intersecting orthogonally, a set of one-dimensional structured Cartesian (horizontal) grids, arranged at equal intervals, parallel to the x_1 coordinate direction, with an another set of one-dimensional structured Cartesian (vertical) grid, arrangedat equal intervals, parallel to the x_2 coordinate direction.

Revised Manuscript Received on February 28, 2020.
***** Correspondence Author
E. Dhananjaya*, Research Scholar, Jawaharlal Nehru Technological University Anantapur, Ananthapuramu, Andhra Pradesh-515002, India. Email: dhanuelisetty@gmail.com
R. Bhuvana Vijaya, Professor and Head, department of Mathematics, Jawaharlal Nehru Technological University Anantapur, Ananthapuramu, Andhra Pradesh-515002, India. Email: bhuvanavijayarachamalla@gmail.com

The grid lines traced parallel to the x_1 and x_2 directions are denoted, by the indices j and i, respectively where, $j = 0.....N_{x_2}$ and $i = 0,.....N_{x_1}$.

The location on the grid lines marked with the filled circles, represent the cell vertices denoted, by the index (i, j).

The nodes on the horizontal grid lines with the index $j = 0$ and $j = N_{x_2}$ represent, respectively the boundary nodes on the bottom and top extremes of the computational domain.

Similarly, the nodes on the vertical grid lines with the index $i = 0$ and $i = N_{x_1}$ represent, respectively the boundary nodes on the left and right extremes of the computational domain. On this particular mesh, it is appropriate to use the horizontal gridlines, to derive the system of compact schemes, for the partial derivatives $\frac{\partial^2 f}{\partial x_1^2}$. Similarly the vertical grid lines are used to derive the system of compact schemes, for the partial derivatives $\frac{\partial^2 f}{\partial x_2^2}$. Thus, by marching line by line along the horizontal and vertical gridlines, the spatial derivative of a function, f could be approximated in a two-dimensional computational domain, subjected to suitable boundary conditions.

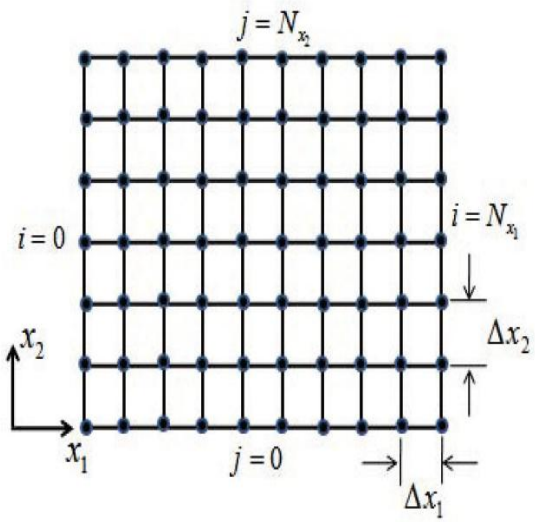

Figure 1.1: A typical two-dimensional structured Cartesian uniform grid

III. COMPACT SCHEMES FOR THE SPATIAL DISCRETIZATION OF LAPLACE AND POISSON EQUATIONS

A system of compact schemes used, to approximate the partial derivative $\frac{\partial^2 f}{\partial x_1^2}$, on the non-boundary nodes, at ψ_i where, $i = 1.....(N_{x_1} - 1)$ as well as the boundary nodes, at ψ_0 and $\psi_{N_{x_1}}$ located along a particular horizontal grid line (shown in Figure 1.2) of a two-dimensional structured Cartesian uniform grid are given by,

$$f''_{\psi_0} + \alpha_L f''_{\psi_1} = \frac{a_L f_{\psi_0} + b_L f_{\psi_1} + c_L f_{\psi_2} + d_L f_{\psi_3} + e_L f_{\psi_4}}{\Delta x_1^2} + o\left(\Delta x_1^3\right) \quad \text{(1.3a)}$$

$$\alpha_i f''_{\psi_{i-1}} + f''_{\psi_i} + \beta_i f''_{\psi_{i+1}} = r\frac{\left(f_{\psi_{i-1}} - 2f_{\psi_i} + f_{\psi_{i+1}}\right)}{\Delta x_1^2} + o\left(\Delta x_1^4\right),\ i = 1.....\left(N_{x_1} - 1\right) \quad \text{(1.3b)}$$

$$f''_{N_{x_1}} + \alpha_R f''_{\psi_{N_{x_1}-1}} = \frac{a_R f_{N_{x_1}} + b_R f_{N_{x_1}-1} + c_R f_{N_{x_1}-2} + d_R f_{N_{x_1}-3} + e_R f_{N_{x_1}-4}}{\Delta x_1^2} + o\left(\Delta x_1^3\right) \quad \text{(1.3c)}$$

Equations (1.3a) - (1.3c) are solved simultaneously, using the known values of the function, f on the boundary nodes, at ψ_0 and $\psi_{N_{x_1}}$ and some guessed values on the non-boundary nodes, at ψ_i where, $i = 1.....\left(N_{x_1} - 1\right)$. The values of the coefficients involved in the equation (1.3) are given in the Table 1.1. These values are obtained from the relations between the coefficients corresponding to each of the equations (1.3a) - (1.3c), derived by matching the Taylor series coefficients of various orders.

The matrix representation of the equation (1.3) is given by,

$$[A_{xx}]F_{xx} = [B_{xx}]f_R + f_{R_1} \quad (1.4)$$

where, A_{xx} and B_{xx} represent the matrices constructed from, collecting the values of the coefficients in the LHS and in the RHS of the system of equations (1.3a) - (1.3c), respectively.

Similarly, F_{xx} and f_R represent the column vectors of the nodal (of both boundary and non-boundary) values in the LHS (of $\frac{\partial^2 f}{\partial x_1^2}$) and in the RHS (of function values)represented, in the system of equations (1.3a) - (1.3c), respectively. The column vector f_{R_1} contains constant values corresponding the near boundary nodes, due to the Dirichlet boundary condition which is imposed on the nodes, along the left and right boundaries of the two-dimensional computational domain. The discrete values in the column vectors F_{xx}, f_R and f_{R_1} are sequenced, with respect to the indices of the nodes, belonging to a particular horizontal grid line, about which the computations are performed.

From equation (1.4), the formula to compute the values of the partial derivative $\frac{\partial^2 f}{\partial x_1^2}$ on the boundary nodes, at ψ_0 and $\psi_{N_{x_1}}$ and on the non-boundary nodes, at ψ_i where, $i = 1.....\left(N_{x_1} - 1\right)$ located on a particular horizontal grid line, of a two-dimensional structured Cartesian uniform grid is deduced as,

$$F_{xx} = [A_{xx}]^{-1}[B_{xx}]f_R + [A_{xx}]^{-1} f_{R_1} \quad (1.5)$$

The calculations in the equation (1.5) involve a tridiagonal matrix inversion and a matrix vector multiplication.

A system of compact schemes used, to approximate the partial derivative $\frac{\partial^2 f}{\partial x_2^2}$, only on the non-boundary nodes, at ψ_j where, $j = 1.....\left(N_{x_2} - 1\right)$ located along a particular vertical grid line (shown in Figure 1.3) of a two-dimensional structured Cartesian uniform grid are given by,

$$f''_{\psi_1} + \alpha_L f''_{\psi_2} = \frac{a_L f_{\psi_0} + b_L f_{\psi_1} + c_L f_{\psi_2} + d_L f_{\psi_3} + e_L f_{\psi_4}}{\Delta x_2^2} + o\left(\Delta x_2^3\right) \quad (1.6a)$$

$$\alpha_j f''_{\psi_{j-1}} + f''_{\psi_j} + \beta_j f''_{\psi_{j+1}} = r\frac{\left(f_{\psi_{j-1}} - 2f_{\psi_j} + f_{\psi_{j+1}}\right)}{\Delta x_2^2} + o\left(\Delta x_j^4\right), i = 2.....\left(N_{x_2} - 2\right) \quad (1.6b)$$

$$f''_{N_{x_2}-1} + \alpha_R f''_{\psi_{N_{x_2}-2}} = \frac{a_R f_{N_{x_2}} + b_R f_{N_{x_2}-1} + c_R f_{N_{x_2}-2} + d_R f_{N_{x_2}-3} + e_R f_{N_{x_2}-4}}{\Delta x_2^2} + o\left(\Delta x_2^3\right) \quad (1.6c)$$

Equations (1.6a) - (1.6c) are solved simultaneously, using the known values of the function, f on the boundary nodes, at ψ_0 and $\psi_{N_{x_2}}$ and some guessed values on the non-boundary nodes, ψ_j at where $j = 1.....\left(N_{x_2} - 1\right)$, The values of the coefficients involved in the equation (1.6) are given in the Table 1.2. These values are obtained from the relations between the coefficients corresponding to each of the equations (1.6a) - (1.6c), derived by matching the Taylor series coefficients of various orders.

The matrix representation of the equation (1.6) is given by,

$$\left[A_{yy}\right] F_{yy} = \left[B_{yy}\right] f_C + f_{C_1} \quad (1.7)$$

where, A_{yy} and B_{yy} represent the matrices constructed from, collecting the values of the coefficients in the LHS and in the RHS of the system of equations (1.6a) - (1.6c), respectively.

Similarly, F_{yy} and f_C represent the column vectors of the nodal (of non-boundary) values in the LHS (of $\frac{\partial^2 f}{\partial x_2^2}$) and in the RHS (of function values) of the system of equations(1.6a) - (1.6c), respectively. The column vector f_{C_1} contains constant values corresponding the near boundary nodes, due to the Dirichlet boundary condition which is imposed on the nodes along the bottom and top boundaries of the two dimensional computational domain. The discrete values in the column vectors F_{yy} , f_C and f_{C_1} are sequenced, with respect to the indices of the nodes, belonging to a particular vertical grid line, about which the computations are performed.

From equation (1.7), the formula to compute the values of the partial derivative $\frac{\partial^2 f}{\partial x_2^2}$ on the non-boundary nodes ,at ψ_j where, $j = 1.....\left(N_{x_2} - 1\right)$ located on a particular vertical grid line, of a two-dimensional structured Cartesian uniform grid is deduced as,

$$F_{yy} = \left[A_{yy}\right]^{-1}\left[B_{yy}\right] f_C + \left[A_{yy}\right]^{-1} f_{C_1} \quad (1.8)$$

The calculations in the equation (1.8) involve a tridiagonal matrix inversion and a matrix vector multiplication.

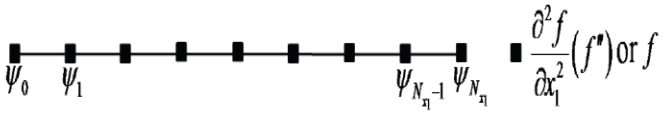

Figure 1.2: One-dimensional structured Cartesian uniform grid used to approximate the partial derivative $\frac{\partial^2 f}{\partial x_1^2}$ on a non-periodic Computational Domain

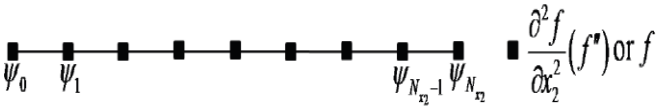

Figure 1.3: One-dimensional structured Cartesian uniform grid used to approximate the partial derivative $\frac{\partial^2 f}{\partial x_2^2}$ on a non-periodic Computational Domain

Table 1.1 : Values of the coefficients in the equations (1.3a) – (1.3c)

Left near boundary node	Interior node	Right near boundary node
$\alpha_L = 11.0$	$\alpha = \frac{1.0}{10.0}$	$\alpha_R = \alpha_L$
$a_L = 13.0$	$\beta = \frac{1.0}{10.0}$	$a_R = a_L$
$b_L = -27.0$	$\gamma = \frac{12.0}{10.0}$	$b_R = b_L$
$c_L = 15.0$	$---$	$c_R = c_L$
$d_L = -1.0$	$---$	$d_R = d_L$

Table 1.2: Values of the coefficients in the equations (1.6a) - (1.6c)

Left near boundary node	Interior node	Right near boundary node
$\alpha_L = -1.0$	$\alpha = \frac{1.0}{10.0}$	$\alpha_R = \alpha_L$
$a_L = 1.0$	$\beta = \frac{1.0}{10.0}$	$a_R = a_L$
$b_L = -3.0$	$\gamma = \frac{12.0}{10.0}$	$b_R = b_L$
$c_L = 3.0$	$---$	$c_R = c_L$
$d_L = 1.0$	$---$	$d_R = d_L$

IV. ALGORITHM TO SOLVE THE FULLY DISCRETIZED LAPLACE AND POISSON EQUATIONS

STEP:1

The compact scheme based interpolated values, of the partial derivative $\frac{\partial^2 f}{\partial x_1^2}$ over the entire boundary and the non-boundary nodes of the two-dimensional computational domain are computed, by solving the equation (1.5) over each of the horizontal grid lines, indexed between $j = 0.....N_{x_2}$

In this computation, the value of the function, f on the boundary nodes located along the vertical grid lines, indexed as, $i = 0$ and $i = N_{x_1}$, respectively (representing for the left and right boundaries) are known, from the given boundary conditions. Likewise, the value of the function, f on the non-boundary nodes, at ψ_i where, $i = 1.....\left(N_{x_1} - 1\right)$ located along each of the horizontal grid lines are assigned, with an initial guess value.

STEP:2

By substituting, the computed values of the partial derivative $\frac{\partial^2 f}{\partial x_1^2}$ and the approximation for the spatial derivative $\frac{\partial^2 f}{\partial x_2^2}$ given by the equation (1.8), into the equations (1.1) and(1.2), the fully discretized form of them, corresponding to a particular vertical grid line are given, respectively by,

$$F_{xx} + \left[A_{yy}\right]^{-1}\left[B_{yy}\right] f_C = G_s - \left[A_{yy}\right]^{-1} f_{C_1} \qquad (1.9)$$

where, G_s is the column vector of the discrete value of the source term of the Poisson equation, on the non-boundary nodes and

$$F_{xx} + \left[A_{yy}\right]^{-1}\left[B_{yy}\right] f_C = -\left[A_{yy}\right]^{-1} f_{C_1} \qquad (1.10)$$

Pre-multiplying the equations (1.9) and (1.10) with the matrix A_{yy} and after further simplification, the algebraic equations to compute the solution of the discretized governing PDE, on a particular vertical line of the two-dimensional Cartesian grid are given, respectively as,

$$\left[B_{yy}\right] f_C = \left[A_{yy}\right] G_s - \left[A_{yy}\right] F_{xx} - f_{C_1} \qquad (1.11)$$

and

$$\left[B_{yy}\right] f_C = -\left[A_{yy}\right] F_{xx} - f_{C_1} \qquad (1.12)$$

Where, the coefficient matrix B_{yy} has a pentadiagonal matrix structure. Equations (1.11) or (1.12) are solved over each of the vertical grid lines, indexed between $i = 1.....\left(N_{x_1} - 1\right)$ Thus, the updated value of the function, f on the entire non-boundary nodes of the computational domain are obtained. The procedure to solve the equations (1.11) or (1.12) involves, a matrix vector multiplication and a vector-vector subtraction in its RHS. The coefficient matrix B_{yy} in its LHS is solved iteratively, using the i-CGSTAB(2) algorithm, as referred in Saad, 1996.

Thus, the equations (1.5) in step 1 and the equations (1.11) or (1.12) in step 2 are solved iteratively, using the above mentioned Gauss-Seidel procedure, along with an under -relaxation strategy. The iterations are continued, until the set convergence, for the true error norm of the numerical solution is attained.

V. TEST PROBLEMS

In this subsection, the higher order spatial accuracy of the developed central difference based compact schemes, for the Poisson and Laplace equations is validated, by solving numerically two test problems. The exact solutions of these problems satisfy the respective governing PDE, subjected to Dirichlet boundary conditions.

VI. PROBLEM1

$$f\left(x_1, x_2\right) = \frac{8}{\pi^3}\sum_{m=1}^{\infty} \frac{\sin\left[\left(2m-1\right)\pi x_1\right]\sinh\left[\left(2m-1\right)\pi\left(x_2 - 1\right)\right]}{\sinh\left[-\left(2m-1\right)\pi\right]/\left(2m-1\right)^3} \qquad (1.13)$$

where, m is the summation index of the series solution. Equation (1.13) represents the exact solution, that satisfies the Laplace equation, restricted over a square domain of $0 \le x_1 \le 1$ and $0 \le x_2 \le 1$. The Dirichlet boundary conditions required to solve this equation are derived, from the given exact solution. A schematic of the computational domain along with the boundary conditions is shown, in the Figure 1.4. The grid sizes chosen to conduct numerical experiment on this problem include, $17\text{x}17, 33\text{x}33, 65\text{x}65, 129\text{x}129$ and $257\text{x}257$. The stopping criteria of the iterative process is defined as, $\left\| f^{k+1} - f^{k} \right\|_{\infty} \le 10^{-20}$. Herein k refers to the iteration index.

VII. RESULT

From the plot of the l_2 norm of the true error, as a function of number of nodes (N) shown, in the Figure 1.5(a), it is observed that, at the set convergence limit, the accuracy of the numerical solution produced, using the compact scheme is higher, compared to the same produced using the second order scheme. In addition, the log-log plot of the l_2 norm of the true error, as a function of number of nodes (N) shown, in the Figure 1.5(b) clearly illustrate the higher order of accuracy of numerical solution produced using the compact scheme.

Similarly, the log-log plot of the l_2 norm of the true error, as a function of number of iterations shown, in the Figure 1.5(c) reveals that, on all the grids chosen for the numerical experiment, in general, the l_2 norm of the true error, of the solution produced, using the 4^{th} order compact scheme is lower, compared to the same produced using the 2^{nd} order conventional scheme.

Also, this particular reduction in the l_2 norm of the true error of the solution attains a steady state, after the chosen convergence limit is reached.

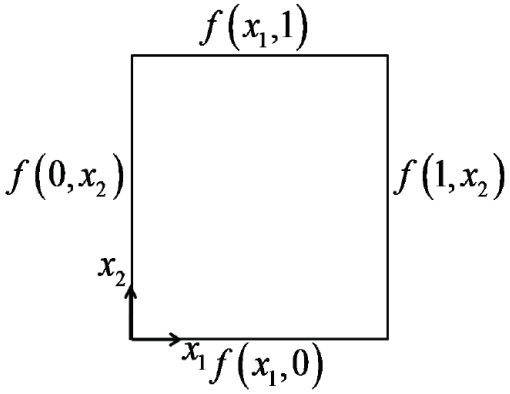

Figure 1.4: A schematic of the computational domain along with boundary conditions used, to solve the two-dimensional Laplace equation

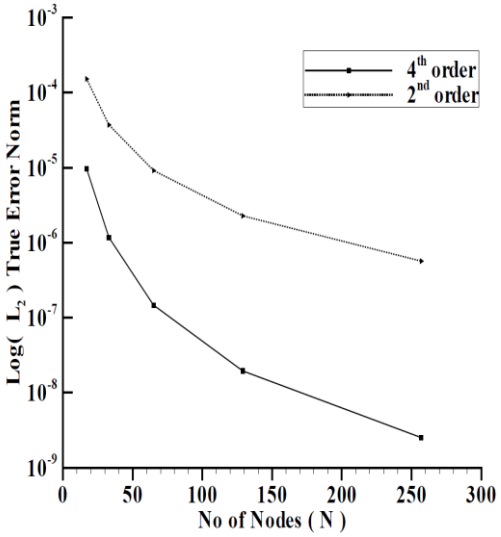

Figure 1.5: (a) Comparison of the grid refinement study of order of accuracy, between compact 4^{th} order and conventional 2^{nd} order schemes.

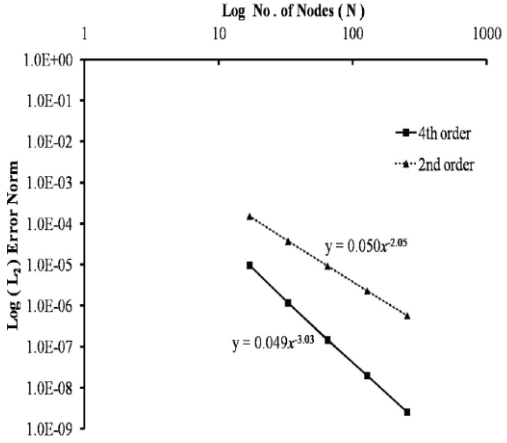

Figure 1.5 (b) Log-Log plot of comparison of the grid refinement study of order of accuracy, between compact 4^{th} order and conventional 2^{nd} order schemes.

PROBLEM 2

$$f(x_1,x_2)=\sin(\pi x_1)\sin(\pi x_2)e^{\pi(x_1+x_2)} \quad (1.14a)$$

$$g(x_1,x_2)=2\pi^2\left(\sin(\pi x_1)\cos(\pi x_2)+\cos(\pi x_1)\sin(\pi x_2)\right)e^{\pi(x_1+x_2)} \quad (1.14b)$$

Equation (1.14a) represents the exact solution, that satisfies the Poisson equation, restricted over a square domain of $0\le x_1\le 1$ and $0\le x_2\le 1$. The Dirichlet boundary conditions required to solve this equation are derived, from the given exact solution. Equation (1.14b) represents the source term of the Poisson equation. A schematic of the computational domain along with the boundary conditions is shown, in the Figure 1.6. The grid sizes chosen to conduct the numerical experiments on this problem include, $17x17, 33x33, 65x65, 129x129$ and $257x257$. The stopping criterion of the iterative process is defined as $\left\| f^{k+1}-f^{k}\right\|_2 \le 10^{-17}$.

Result

From the plot of the l_2 norm of the true error, as a function of number of nodes (N) shown, in the Figure 1.7(a), it is observed that, at the set convergence limit, the accuracy of the numerical solution produced, using the compact scheme is higher, compared to the same produced using the second order scheme. In addition, the log-log plot of the l_2 norm of the true error, as a function of number of nodes (N) shown, in the Figure 1.7(b) clearly illustrate the higher order of accuracy of numerical solution produced using the compact scheme.

Similarly, the log-log plot of the l_2 norm of the true error, as a function of number of iterations shown, in the Figure 1.7(c) reveals that, on all the grids chosen for the numerical experiment, the l_2 norm of the true error of the solution, produced using the compact 4^{th} order scheme is lower, compared to the same based on the 2^{nd} order conventional scheme. Also, this particular reduction in the l_2 norm of the true error of the solution attains a steady state, after the chosen convergence limit is reached.

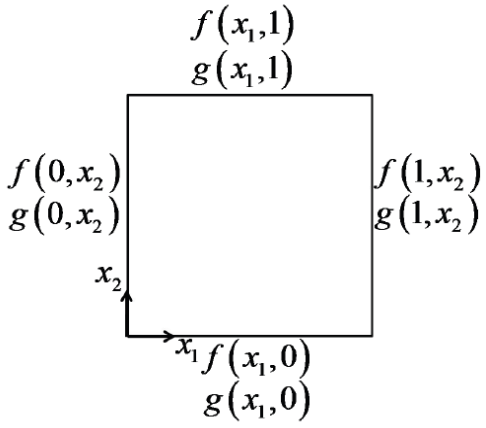

Figure 1.6: A schematic of the computational domain along with boundary conditions used, to solve the two-dimensional Poisson equation

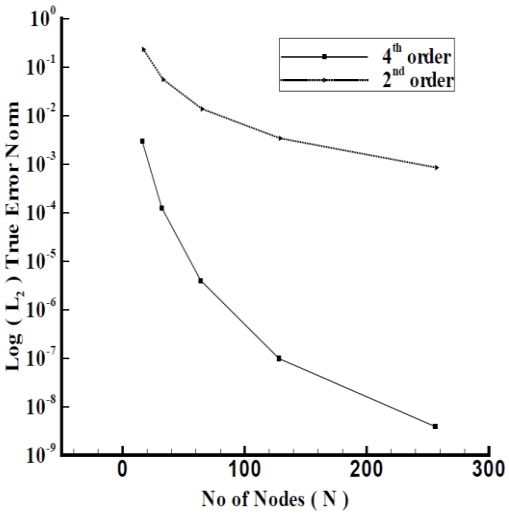

Figure 1.7: (a) Comparison of grid refinement study of order of accuracy between compact 4^{th} order and conventional 2^{nd} order schemes.

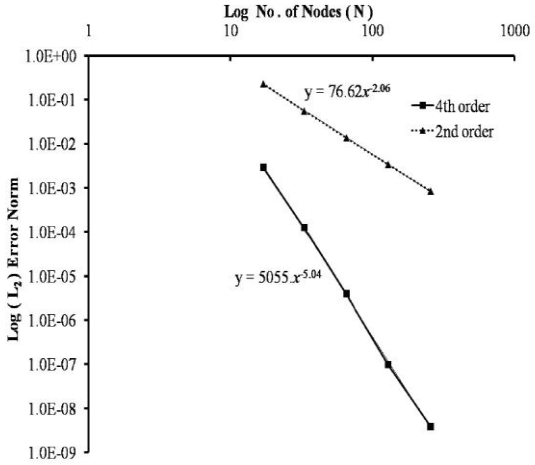

Figure 1.7: (b) Log-Log plot of comparison of grid refinement study of order of accuracy between compact 4^{th} order and conventional 2^{nd} order schemes.

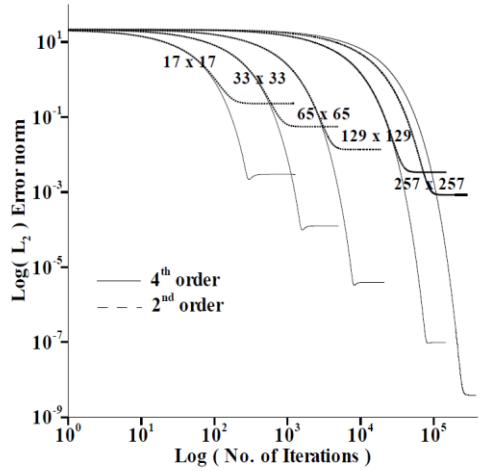

Figure 1.7: (c) Comparison of rate of convergence of solution between compact 4^{th} order and conventional 2^{nd} order schemes.

VIII. CONCLUSION

It is observed that, the accuracy of the numerical solution produced, using the compact scheme is higher, compared to the same produced using the second order scheme. The l_2 norm of the true error, of the solution produced, using the 4^{th} order compact scheme is lower, compared to the same produced using the 2^{nd} order conventional scheme. Also, this particular reduction in the l_2 norm of the true error of the solution attains a steady state, after the chosen convergence limit is reached.

REFERENCES

1. D. Gilbarg and N. Trudinger, Elliptic Partial Differential Equations of Second Order, Springer Verlag, Berlin, 1983.
2. Jost, J. (2002), Partial Differential Equations, New York: Springer-Verlag.
3. Thomas, Numerical Partial Differential Equations: Finite Difference Methods. Springer-Verlag, New york, 1998.
4. Chang, H.-R. andH. N. Shirer (1985). Compact spatial differencing techniques in numericalmodeling. Monthly Weather Review, 113, 409–423.
5. E, W. and J. G. Liu (2001). Projection Method, Part III: Spatial discretization on the staggered grid. Mathematics of Computation, 71(237), 27–47.
6. Kampanis, N. A. and J. A. Ekaterinaris(2006). A staggered grid, high-order accurate method for the incompressible Navier-Stokes equations. Journal of Computational Physics, 215, 589–613.
7. Knikker, R. (2008). Study of a staggered fourth-order compact schemes for unsteady incompressible viscous flows. International Journal for Numerical Methods in Fluids.
8. Strikwerda, J. C. [2004] Finite Difference Schemes and Partial Differential Equations, 2nd edn. (SIAM, Philadelphia).
9. S. K. Lele, Compact Finite Difference Schemes with Spectral-Like Resolution, J. Comput. Phys., vol. 103, pp. 16–42, 1992.
10. K. Mahesh, A Family of High Order Finite Difference Schemes with Good Spectral Resolution, J. Comput.Phys., vol. 145, pp. 332–358, 1998.
11. X. Zhong, High-Order Finite Difference Schemes for Numerical Simulation of Hypersonic Boundary-Layer Transition, J. Comput. Phys., vol. 144, pp. 662–709, 1998.
12. M. Yanwen, F. Dexun, T. Kobayashi, and N. Taniguchi, Numerical Solution of the Incompressible Navier-Stokes Equations with an Upwind Compact Finite Difference Scheme, Int. J. Numer.Meth.Fluids, vol. 30, pp. 509–521, 1999.
13. Y. Li and M. Rudman, Assessment of Higher-Order Upwind Schemes Incorporating FCT for Convection Dominated Problems, Numer. Heat Transfer B, vol. 27, pp. 1–21, 1995.
14. T. K. Sengupta, G. Ganeriwal, and S. De, Analysis of Central and Upwind Compact Schemes, J. Comput.Phys., vol. 192, pp. 677–694, 2003.
15. Sengupta, T. K., G. Ganeriwal, and S. De (2003). Analysis of central and upwind compact schemes. Journal of Computational Physics, 192, 677–694.
16. You, D. (2006). A high-order Padé ADI method for unsteady convection-diffusion equations. Journal of Computational Physics, 214, 1–11.

AUTHORS PROFILE

E Dhananjaya, Research Scholar, Jawaharlal Nehru Technological University Anantapur, Anantapuramu. He completed his Master of Technology in Industrial Mathematics & scientific Computing From Indian Institute Of Technology, Madras (IIT Madras). He also qualified Top Level National Examinations Like GATE, CSIR.. He is working as lecturer in Mathematics, Government Model Residential Polytechnic, Madanapalle, Andhra Pradesh.

R. Bhuvana Vijaya, Completed her Doctoral programe in Sri Krishnadevaraya University. She has many number of International and National Journals. She is presently working as Professor and Head, department of Mathematics, JNTU college of Engineering, Ananthapuramu.